Effect of pH and nanoclay content on the morphology and physicochemical properties of soy protein/montmorillonite nanocomposite obtained by extrusion

M. Felix[a]*, I. Martinez[b], A. Romero[a], P. Partal[b], A. Guerrero[a]

[a]*Departamento de Ingeniería Química, Universidad de Sevilla, Facultad de Química, 41012 Sevilla, Spain*

[b]*Departamento de Ingeniería Química, Química Física y Ciencia de Materiales, Universidad de Huelva, Facultad de Ciencias Experimentales, 21071 Huelva, Huelva.*

*M. FELIX

Departamento de Ingeniería Química,

Universidad de Sevilla, Facultad de Química,

41012 Sevilla (Spain)

E-mail: mfelix@us.es

Phone: +34 954557179; Fax: +34 954556441.

Abstract

The present work attempts to clarify the influence of montmorillonite nanoclay content and pH on the mechanical properties of extruded soy protein nanocomposites. The mechanical behaviour is dominated by the formation of positive synergies between protein and nanoclay above a nanoclay concentration threshold. Moreover, the presence of nanoclay can improve water uptake. The pH also exerts a strong influence on mechanical and water absorption properties, although montmorillonite tend to reduce this effect.

Eventually, this study put forward the feasibility of using a combination of soy protein and montmorillonite to obtain potentially attractive biodegradable nanocomposite materials, processed by means of a simple and easily scalable twin-screw extruder.

Keywords:

Bioplastic; Extrusion; nanocomposite; Protein Interactions; Rheology; Tensile strength test

1. Introduction

New studies have been devoted to developing new protein-based materials, able to replace fossil-based polymer for high quality applications such as superabsorbents, barrier properties or controlled release of active ingredients [1]. The development of superabsorbent biopolymers requires an in-depth knowledge of the physical, chemical and functional properties of the proteins to be used, as well as of the processing techniques for the polymeric matrixes (extrusion, compression or injection moulding). The formulation and processing of these materials must be evaluated in terms of their physicochemical properties.

A superabsorbent material usually retains around twenty times its own weight in water. After absorption, the aqueous fluid is not free to flow out of the molecular network of the “hydrogel”. As a result, the fluid is like a state of matter intermediate between liquid and solid, exhibiting properties of both. The mechanical responses of these systems directly result from interactions of the polymer network with water [2].

To obtain protein-based biopolymers, we require a highly hydrophilic protein, such as soy protein isolate (SPI), and this type of protein has already been demonstrated to be suitable for creating bioplastics in combination with a proper plasticiser, exhibiting a high water uptake

capacity [3–5]. SPI proteins were initially classified by ultracentrifugal analysis into four fractions: 2S, 7S, 11S, and 15S [6]. The l1S fraction consists primarily of a single protein and represents about 60% of the total protein in SPI. This fraction is composed of an acidic polypeptide (about 38 kDa) and a basic polypeptide (about 20 kDa) linked by a single disulphide bridge [7]. The second most abundant protein in SPI is the 7S fraction, which represents about 35% of the total soy protein [6].

Lamellar nanofillers have been postulated to improve mechanical and barrier properties of bioplastics. Natural Montmorillonite (MMT-Na^+) is a type of clay mineral widely used in polymer science as filler. It is widely available in nature as micron-size tactoids. These tactoids consist of several hundred individual platelets held together by electrostatic forces, which are forming stacks or groups of stacks, with approximately 1-nm gap between each platelet, and the structure is supported by Van der Waals interactions [8].

The incorporation of this type of materials leads to an increase in water uptake capacity, and, at the same time, enhances the mechanical properties of the hydrogel (especially strength and stiffness) [9]. However, the dispersion of such nanoclay platelets or stacks within a polymer structure is complex and its efficient dispersion in biopolymer matrices is a key problem in the development of biodegradable nanocomposites, in which it is desirable for the material to be exfoliated to improve nanocomposite properties. In this context, melt intercalation in an extruder is one of the most promising techniques for preparing biopolymer nanocomposites because of its ease and versatility. Layered clays (6-13 μm) are typically sheared and peeled apart into platelets (1-10 nm) due to high shear mixing inside the extruder [8]. Notably, extrusion is one of the most important processing techniques to produce plastics on a commercial scale.

Various behaviours in polymer-MMT blends have been described in the literature depending on the polymer-clay interactions taking place. If the interactions are very weak, tactoids remain unaltered in the polymer matrix, no true nanocomposite is formed, and as a consequence, mechanical properties of the resulting material are markedly different to those of the original polymer. When there is moderate interaction, the clay interlayer expands, and under these conditions, polymer chains penetrate into the gaps between plates, leading to an intercalated structure. On the other hand, if the original tactoid structure is lost during processing, we can assume that the nanoclay has taken on an exfoliated structure, where clay platelets become dispersed into the polymer matrix, and this leads to the greatest improvements in polymer

performance [10–13]. This behaviour is due to the higher difference in surface-to-volume ratio between the clay and the polymer matrix, characteristic of nanoparticles [1].

To enhance the nanoclay dispersion in polymer matrices and improve the properties of the resulting nanocomposite, various processing conditions such as shear rate and pH level should be optimised [8]. Basically, proteins have a net positive charge when the pH is lower than the isoelectric point (IEP) and a net negative charge when the pH is higher than the IEP [3]. Electrostatic repulsions between protein molecules occur at pH values away from the IEP. As a consequence, tuning the pH can be used as an alternative method to improve the functional properties, such as film-forming, gelling, emulsifying, and foaming properties of many proteins (e.g. gelatin) [14]. Hence, the physical properties of protein-based composite will be highly influenced by the pH. The proteins with charged residues are more likely to interact with hydrophilic nanoclays at different degrees. Cloisite Na^+, an hydrophilic nanoclay which is frequently used in bio-based nanocomposites, is a cationic clay mineral with a negative charge on its outer structure [15].

Thus, pH may directly affect the interaction and distribution of nanoclays in soy protein matrix. Nevertheless, there is little data on the effect of pH on the properties of films in which nanoclays have been incorporated [16].

The overall objective of this work was to develop and characterize SPI/MMT-Na^+ biodegradable nanocomposite plastic materials, plasticised with glycerol (GL) by means of lab-scale extruder processing. Effects of the pH and MMT content on the structure and properties (rheological, mechanical and water uptake) of SPI/MMT-Na+ nanocomposite plastics were investigated. In addition, X-ray diffraction and transmission electron microscopy (TEM) were used to investigate the behaviour of clay dispersion in the nanocomposite.

2. Experimental

2.1. Materials

Soy Protein Isolated (SPI) Supro 500E was supplied by Protein Technologies International (Leper, Belgium). The protein content was determined in quadruplicate as % N x 6.25 using a LECO CHNS-932 nitrogen micro analyser (Leco Corporation, St. Joseph, MI, USA) being 91±0.5 wt.%, the ash and the moisture content were also determined according to A.O.A.C. methods [17], being 5.2±0.1 and 3.7.0±0.5wt.%, respectively. Glycerol (GL), used as plasticizer, was purchased from Sigma-Aldrich (St. Louis, Missouri, USA). The pH modifiers, Ethanolamine and 4-Dodecylbenzenesulfonic acid, were also purchased from Sigma-Aldrich

(St. Louis, Missouri, USA). The nanoclay introduced was Cloisite® Na^+ (MMT-Na^+). It was obtained from Montmorillonite, and manufactured by Southern Clay Products, Inc. (USA).

2.2. Sample preparation

Blends with constant SPI/GL ratio (50/50) were manufactured by means of extrusion process. This ratio protein/plasticiser was in accordance with previous studies for superabsorbent materials obtained by injection moulding [5]. The pH was modified by adding 2 wt.% of organic basic or acid to the glycerol, and the MMT was added after a previous hand-mixing in a proper ratio whit the SPI. One of the limitation of adding aqueous solution of strong acid or basis (such as NaOH, NH_3, HCl or H_2SO_4) is the incorporation of water as plasticiser, which has a strong influence even in a short amount [18]. For this reason, the acid and the basis selected were organic compounds without any plasticiser activity reported until nowadays. The compounds selected were: 4-dodecylbenzenesulfonic acid and ethanolamine, as acid and basis, respectively. The pH of the final GL was 1.5 and 9.5, after adding the acid and the basis, respectively. The pH of the blends before extrusion were also controlled, the pH values obtained were 6.7 and 9.5, respectively (whereas the pH of the reference system is 8.1).

The twin-screw extruder used was the EuroLab 16 (ThermoScientific, Massachusetts, USA). The diameter of this extruder is 19 mm and the length/diameter ratio (L/D) is 40. In addition, this extruder is able to control the temperature of 11 heads at the barrel, including the die. The selected temperature profile is shown in Table 1. This conditions are similar to those used for protein-based extruded materials [8,19,20]. Other temperatures profiles were evaluated. However, lower temperatures led to low-processed materials, characterised by softness and brightness. On the other hand, higher temperatures yield materials which are not easily processable and, as a consequence, these materials produce frequently overloads in the extruder. The selected processing conditions produce suitable materials, being the extruder torque per shaft about the 70-80 % of the maximum value allowed (12 N·m). Two feeding units, a peristaltic liquid pump and a powder dispenser, were used for the addition of liquids and solids, respectively.

Finally, the die selected has the sheet-shape (2 x 50 mm). Then, in order to obtain standardised probes the sheet was die-cut with the shape of the Dumpbell for tensile strength [21] or rectangular for DMA, torsion, water uptake and X-Ray measurements. Thus, several systems were obtained, all of them denoted as SPI, without pH modification (containing from 0 to 9

wt.% of MMT) and with the pH modification of the plasticiser (containing 0 and 6 wt.% of MMT).

2.3. Characterization

2.3.1 Dynamic Mechanical Analysis (DMA).

Tension

DMA tests were carried out with a Seiko DMS 6100 (Seiko Instruments, Japan), on rectangular probes using oscillatory tension tests. All the experiments were carried out at constant temperature (30 ºC) and strain (between 0.01 and 0.3 %, within the linear viscoelastic region). The selected frequency range was from 0.0628 to 62.8 rad/s.

Torsion

DMA tests were performed with a Physica MCR 302 (Anton-Paar, Graz, Austria) in torsion mode. Frequency sweeps were carried out at a constant temperature (30 ºC) and a stress of 800 Pa (within the linear viscoelastic region). The selected frequency range was from 0.01 to 16 rad/s.

2.3.2. Tensile tests

Tensile tests were performed by using a Shimadzu AG-IS testing machine (Kioto, Japan), according to ISO 527-2:1993 for Tensile Properties of Plastics [22]. Tensile stress and elongation at break were evaluated from at least five replicates for each product using type IV probes and an extensional rate of 10 $mm \cdot min^{-1}$ at room temperature.

2.3.3. Water uptake capacity.

Water uptake of bioplastics was determined following the ASTM D570 norm (ASTM D570-98, Standard test Method for Water Absorption of Plastics) [23] using at least three 60×10×1 mm specimens immersed in distillate water for 2h or 48 h at room temperature.

2.3.4. X-Ray Diffraction (XRD).

XRD studies of the composite specimens were carried out using a D8 Discover (BRUKE, Massachusetts, USA) (40 kV, 30 mA) equipped with Cu Kα radiation (λ=0.154 nm). The scanning range (2θ) was from 2 to 30°, and the step size was 0.05°.

The clay gallery separation or d-spacing was calculated from Bragg's law using XRD results as shows Eq. 1 [24]:

$$d = n\lambda/2sin\theta \quad (1)$$

where d is the spacing between layers of the clay, **n** is a whole number, λ the wavelength of X-ray (1.511 Å) and θ the angle at the maximum point of the mean peak in the spectra.

2.3.5. Transmission Electron Microscopy (TEM)

Specimens for TEM observations were cut from nanocomposite blocks at room temperature, using an EM UC7 Ultramicrotome (Leica, Wetzlar, Germany), equipped with a glass knife, to obtain sections with thickness between 70 and 90 nm. Transmission electron images were taken with a Libra 120 microscope (Zeiss, Oberkochen, Germany) at an acceleration voltage of 80 kV.

3. Statistical analysis

At least three replicates of each measurement were carried out. Uncertainty was determined by means of standard deviations.

4. Results and Discussion

4.1. Linear viscoelastic properties

Influence of MMT-Na^+ concentration

Figure 1 shows results from dynamic mechanical analysis for systems with the same protein/plasticiser ratio, different concentrations of MMT-Na^+ (0, 1, 2, 3, 6 and 9 wt.%), at the reference pH (pH of blends of 8.1 related to the value of soy dissolved in glycerol). Mechanical spectra are shown in Figure 1A. Considering the profiles obtained, the viscoelastic response is characteristic of a solid-like behaviour, with the elastic modulus (E') being greater than the viscous modulus (E''), and additionally, they evolve almost in parallel over the whole frequency range (from 0.06 to 64 rad/s). As can be observed, both moduli (E' and E'') decrease at first, when a small amount of MMT-Na^+ (1 wt.%) is added. However, when the concentration of nanoclay exceeds a certain amount (around 2 wt.% of MMT), both moduli increase, that is, there is a threshold concentration for which there is a positive contribution of the nanoclay to the protein network structure [25].

Several models have been postulated to explain network formation of a solid in a liquid, one of the most widely used being the percolation model. This model has been useful to explain the percolation threshold in molten polymers with nanocarbon tubes [26–29], exhibiting remarkable changes in both electrical conductivity and rheological properties. However, this parameter has

been used not only in molten polymers, but also in polymers in a solid state at room temperature [30]. In filled polymers, beyond a critical concentration of filler particles (called the percolation threshold), particles can touch each other and have van der Waals interactions between them, thus leading to stronger reinforcement of the structure. A mathematical treatment has been developed to determine the threshold above which the nanoclay have a positive effect on mechanical properties of the nanocomposite. According to the procedure followed by Fernandez, Landa et al. [31], the values of E' (elastic modulus at a given MMT %) and E_0' (elastic modulus in absence of MMT) are taken for the lowest frequency, 0.01 Hz (ca. 0.06 rad/s). Then, they are divided to obtain the ratio $[E'/ E_0']_{0.01}$. The values for this ratio are plotted vs. $(\phi - \phi_c)$, where ϕ is the concentration of nanoclay and ϕ_c is the concentration threshold. Finally, the data are fitted to a power law equation that can be applied when $\phi > \phi_c$ (Eq. 2):

$$\left[\frac{E'}{E_0'}\right]_{0.01} = (\phi - \phi_c)^t, \qquad (2)$$

where *t* is the power-law exponent, which is a fitting parameter. This equation makes reference to an analogous rheological percolation threshold for the penetration of one solid into another, based on dynamic viscoelastic properties.

The elastic modulus for each system at 0.01 Hz (or 0.06 rad/s) divided by E_0 is plotted in Figure 1B versus protein concentration. Additionally, the values for $\left[\frac{E'}{E_0'}\right]_{0.01}^{1/t}$ obtained after fitting the experimental values to Eq. (2) are plotted vs. ϕ for $\phi > \phi_c$. Interestingly, the best fit was obtained for an exponent, t, fairly close to 1, with a percolation threshold concentration ϕ_c = 1.6 wt.%. Although the percolation threshold is similar to values obtained by other authors for segregated networks of micro or nanoparticles into molten polymers [27,29], the values for parameter t are lower than those found in the literature that typically range between 1.6 and 2 [32]

Influence of pH

The aim of the experiments reported in this section was to evaluate the mechanical properties of biopolymer nanocomposites containing GL at different pH values. The pH value of the GL was modified as explained in the experimental section. Furthermore, the influence of the addition of 6 wt.% MMT-Na^+ nanoclay was also evaluated at different pH values.

Figure 2 shows the rheological characterisation of probes at the selected pH values (6.7, 8.1 and 9.5), with 6 wt.% MMT-Na^+ and without nanoclay, from frequency sweep tests in the

torsion mode. The mechanical spectra obtained were plotted in Figure 2A. These results reveal a decrease in modulus when GL pH changes; on the other hand, the slope of G' does not seem to be frequency dependent, which suggests (before considering tan δ profiles) that the solid character of all studied systems remains unaltered within the overall frequency interval studied. After introducing the MMT-Na^+, however, the elastic and viscous moduli are markedly higher, always being higher than the values obtained without MMT-Na^+.

Additionally, tan δ has been plotted in Figure 2B. As may be observed, in absence of MMT-Na^+ is the system without pH-adjustment which exhibits the most solid-like character, tan δ being the lowest. Increasing or decreasing the pH tends to reduce the solid-like characteristics, which may suggest an improvement in the processability of nanocomposite materials, and may be related to a less crosslinked polymer network. This effect is more apparent when the pH is decreased. However, the inclusion of the nanoclay at the studied concentration changes the mechanical behaviour of the systems. Specifically, whereas tan δ increases with frequency in systems without MMT-Na^+, G' is higher in systems containing MMT-Na^+ at low frequencies. The mechanical spectra seem to have shifted, which according to Ferry [33] reflects a transition from a glassy to a crystalline polymer.

4.2. Mechanical characterisation

Influence of MMT-Na^+ concentration

Mechanical characterisation of soy-based extruded nanocomposites was carried out by means of tensile strength measurements. Figure 3A shows the influence of the MMT concentration. Parameters from the stress-strain curve (maximum stress, σ_{max} , strain at break,ε, and Young's modulus, E) have been plotted for the control probe (0 wt.% MMT-Na^+) and probes containing MMT-Na^+ (1, 2, 3, 6 and 9 wt.%). As may be observed in this figure, parameters from the stress-strain curve are in accordance with the data from the mechanical spectra shown in Figure 1B. Systems containing a small amount of MMT-Na^+ (below 3 wt.%) exhibit lower values of all parameters. However, a positive synergy effect seems to take place for a concentration of nanoclay higher than 2 wt.%, MMT-Na^+, giving rise to an increase in the maximum stress and Young's modulus (these being c.a. 2.5 and 2 times higher at 9 wt.%, respectively), while the strain at break decreases from 40 to 20%. This behaviour, occurring above the estimated percolation threshold, is easy to understand from a qualitative point of view as hard, non-deformable fillers introduced into the protein matrix tend to reduce the flexibility (increasing the brittleness) of protein chains, thereby leading to a more rigid structure.

Influence of pH

Subsequently, experiments exploring the influence of pH were carried out and the results are plotted in Figure 3B. This figure shows parameters from the stress-strain curve (maximum stress, strain at break and Young's modulus) for probes containing 0 and 6 wt.% MMT-Na^+ as a function of pH. As may be observed in this figure, in absence of MMT-Na^+ the strain at break passes through a minimum value at intermediate pH, which corresponds to a maximum value for both the Young's modulus and the maximum stress. All these results reflects that any modification of pH (reduction or increase) from the original value (8.1), which involves an increase in the charges of the plasticiser being either positive or negative, leads to a weakening of the microstructure of the specimen.

In contrast, the addition of nanoclay leads to more rigid nanocomposite materials, since maximum stress and Young's modulus increase, whilst the strain at break decreases. In any case, the above-mentioned pH-induced weakening effect tends to loss significance, particularly for the strain at break. Thus, in presence of MMT-Na^+, the only significant effect observed corresponds to σ_{max} and E at the highest pH value. These results seem to be a consequence of the structure of the nanoclay found for these composite materials above the percolation threshold (e.g. at 6 wt.% MMT-Na^+). Thus, once again the mechanical response is controlled by the presence of nanoclay.

4.3. Water uptake capacity

Influence of MMT-Na^+ concentration

Figure 4 shows the water uptake capacity for all systems studied. Figure 4A deals with the influence of MMT concentration. Thus, the water uptake capacity has been plotted in this figure for the reference system (bioplastic from extruded soy, containing 0 wt.% MMT-Na^+), and nanocompoistes materials, containing 1, 2, 3, 6 and 9 wt.% MMT-Na^+. As a general rule, the final water uptake after 48 h increases with nanoclay content. However, when the concentration of MMT is below 2% (i.e. the percolation threshold), a soft decrease in water uptake takes place. This trend changes above the percolation threshold and the increase in MMT induces an increase in water uptake. Additionally, the incorporation of nanoclay slows the kinetics of absorption, since the water uptake after 2h is lower until reach a plateau value. This behaviour has previously been observed in bioplastics containing exfoliated nanoclay [34,35], being related to the creation of a structure which gives a tortuous pathway for fluid transport. In this

303 way, the penetration and diffusivity of water molecules is restricted, resulting in a reduction in
304 the rate of absorption, but not affecting the final water adsorption [34]. Moreover, the trend
305 observed for water uptake after 48 hours is similar to that one found for mechanical properties.
306 Hence, while the total water uptake was found to be slightly lower in systems containing 1 and
307 2 wt.% MMT-Na^+, water uptake was higher for the systems containing more than 2 wt.%
308 nanoclay (i.e. above the percolation threshold).

309 As for the influence of GL pH, Figure 4B shows the water uptake for probes containing both
310 nanoclay concentrations, none and 6 wt.% MMT-Na^+, and the GL was used with and without
311 pH modification. A comparison among systems without nanoclay reveals markedly higher
312 water uptake at 2 and 48 h when the pH is modified. This significant increase may be related to
313 less protein crosslinking, which also causes the above-mentioned lower mechanical properties.
314 This behaviour is also related to swelling properties, which are higher for systems whose pH has
315 been modified than for the system at the initial pH value [36]. This explanation is in accordance
316 with the results of loss of soluble matter, showing greater loss in systems after pH modification.
317 This may also be a consequence of the lower level of crosslinking, since the solubility of
318 proteins increases when the crosslinking decreases, and of the weaker protein-plasticiser
319 interactions, which are less able to hold the soluble matter. Furthermore, this result may also be
320 related to protein unfolding and opening of the structure which takes place far from the IEP at
321 which the protein powder has been obtained [37].

322 A simple observation of the system containing 6 wt.% MMT-Na^+ reveals a significant
323 increase in water uptake compared to the reference system (without MMT-Na^+ and at reference
324 pH), especially for the system at a higher basic pH value, which maintains the mechanical
325 properties and increases the water uptake to 100% (twice the initial value). In addition, the
326 incorporation of nanoclay slows the kinetics of the absorption (water uptake at 2 h being lower,
327 but the final water uptake at 48 h being higher).

328 Lastly, the loss of soluble matter is lower for systems containing 6 wt.% MMT-Na^+ than the
329 systems without MMT-Na^+, this difference being much greater for systems after pH
330 modification. Hence, the loss of soluble matter is not only related to the inclusion of inert
331 MMT-Na^+, but also to the interactions among protein chains and nanoclay or plasticizer
332 molecules.

333 4.4. Structural characterisation

In order to determine the internal structure of the materials, samples were analysed by X-ray diffraction (XRD). Figure 5 shows XRD diagrams for all the systems studied: Figure 5A illustrates the influence of nanoclay concentration, whereas Figure 5B shows the influence of pH.

First of all, one useful feature of this diagram, is that it allows us to characterise the nanoclay exfoliation. The presence of nanoclay is desirable because of the ways they may modify the structure and mechanical properties of the nanocomposites. The XRD diagram for the MMT-Na^+ powder reveals seven peaks, in accordance with previous results from other authors [38,39]. The absence of these peaks in the nanocomposites indicates the separation of clay platelets, which suggests occurrence of exfoliation, at least partially.

Results from XRD reveal that among the systems containing MMT-Na+ only those corresponding to the higher concentrations (6 and 9 wt.% nanoclay) exhibit most of the peaks of the pristine nanoclay (being evident for the peak at θ around 22.5º). However, the angles of the peaks are slightly displaced, indicating a certain increase in the interlayer distance. Hence, It seems that systems are somehow intercalated with a certain degree of exfoliation.

In addition, a detailed study of the SPI XRD may also indicate the structure of the protein. Specifically, the two main peaks present in the SPI have been previously related to the main protein fractions present in the protein powder (fractions 7S and 11S), the first peak being caused by the 7S fraction and the second peak by the 11S fraction (the pattern of proteins belonging to the α-helix and β-sheet present in the tertiary structure of proteins). Furthermore, the intensities of these peaks have also been related to the amount of these fractions. In accordance with these premises, the SPI powder used in this study exhibits both peaks, but certain changes can be observed when it is processed.

Firstly, the peak corresponding to the 7S fraction is almost completely absent for the systems containing no MMT-Na^+ or only a small amount. The decrease is especially relevant for the system at a basic pH, where there is a complete absence of the peak for this fraction. These results are not in accordance with Peng et al. [6], who reported the transformation of the 11S fraction into 7S and 2S. However, these experiments were carried out in water solution and not in solid phase.

Figure 6 shows images obtained by TEM from samples without MMT-Na^+ (Fig. 6A), as well as with MMT-Na^+ (Figures 6B and 6C). A fast overview of these pictures reveals noticeable differences among systems containing or non-containing nanoclay; small clay platelets with

exfoliated layers and some intercalated clay structure are visible in Figure 6B and 6C but not in Figure 6A. The presence of spherical globules together with the absences of platelets in Figure 6A, indicate an extensive region where protein and plasticiser are forming a polymer matrix, with the presence of some spherical protein aggregates. Despite the fact that TEM images obtained from bioplastics of films are scarce, some authors have found a similar amorphous structure for bioplastics [11] or protein-based films [40]. However, the appearance of platelets in Figures 6B and 6C indicate that the addition of nanoclay (6%wt.) introduces noticeable structural changes. In fact, both figures show that nanoclay platelets are connected, which is consistent with the formation of a nanoclay network after a concentration of MMT-Na^+ higher than the above-mentioned percolation threshold.

The orientation of nanoclay platelets or stacks found in this case is different to that one obtained for egg albumen bioplastics, where MMT-Na^+ nanoclay was present in the form of large and stripe-shaped aggregates with a defined orientation (arranged almost parallel to each other) [11]. However, in the present case, the formation of the nanoclay network can also justify the increase in mechanical properties found (10). The low magnification TEM image provided in Figure 6C shows that the delaminated silicate lamellas in the bioplastic are further randomized, disordered and shifted during the extruding process. The dimensions of the silicate layers are diminished to about 1 nm in thickness (Figure 6C). It indicates the layered MMT-Na^+ is exfoliated by the soy protein molecules in the sample. However, some of the layered MMT-Na^+ tactoids are intercalated with a d-spacing of about 5-6 nm (Figure 6B and 6C) which would correspond to the gallery size between platelets. These thickness values seem to describe an intercalated structure instead of fully exfoliated, as the platelets appear to exhibit some spatial ordination and proximity between them. Similar results have been found in similar systems (17).

5. Conclusions

A percolation threshold is found for MMT-Na^+ filled nanocomposites at a concentration close to 2 wt.%. In particular, mechanical and water uptake properties are highly affected by this event. After adding MMT-Na^+ at a concentration higher than the percolation threshold, the mechanical properties are dominated by the nanoclay network structure, since protein chains have less mobility; on the other hand, water uptake capacity is much higher than in the reference system.

A change in the pH value of the plasticiser from the initial value, by adding either an organic acid or an organic base, produces a noticeable change in mechanical properties. Both effects lead to nanocomposites with a higher plastic deformation, since polymer chains are able to slide easily, this being manifested by a lower Young's modulus and maximum stress. They also yield a much higher strain at break. Both effects also affect the water uptake capacity, since they lead to lower protein crosslinking that allows the polymer to swell in a greater extent. As a result, a higher water uptake capacity is in both cases achieved. When nanoclay is added above the percolation threshold concentration, not only mechanical properties and water uptake capacity of the bioplastic specimens increase, but also their rheological properties are improved, shifting from a glassy behaviour (in absence of nanoclay) to a crystalline-like polymer response. TEM images indicate the partial exfoliation of nanoclay platelets, as well as the formation of a nanoclay-based network.

In summary, the results obtained in this study put forward the feasibility of using a combination of SPI and MMT-Na^+ to obtain potentially attractive biodegradable nanocomposite materials, processed by means of a simple and easily scalable twin-screw extruder.

6. Acknowledgements

This work is part of a research project sponsored by Andalousian Government, (Spain) (project TEP-6134) and by "Ministerio de Economía y Competitividad" from Spanish Government (Ref. CTQ2015-71164-P). The authors gratefully acknowledge their financial support. The authors also acknowledge to the Microscopy and X-Ray Services (CITIUS-Universidad de Sevilla) for providing full access and assistance to the D8 Discover and Libra 120 equipment, respectively. In addition, the authors gratefully acknowledge Asunción Fernández for her technical support in the Microscopy Service.

7. References

[1] Peelman N, Ragaert P, De Meulenaer B, Adons D, Peeters R, Cardon L, et al. Review: Application of bioplastics for food packaging. Trends Food Sci Technol 2013;32:128–41.

[2] Gross JR. The Evolution of Absorbent Materials. In: Lisa B-P, Ronald SH, editors. Stud.

Polym. Sci., vol. Volume 8, Elsevier; 1990, p. 3–22.

[3] Liu WJ, Misra M, Askeland P, Drzal LT, Mohanty AK. “Green” composites from soy based plastic and pineapple leaf fiber: fabrication and properties evaluation. Polymer (Guildf) 2005;46:2710–21.

[4] Song F, Tang D-L, Wang X-L, Wang Y-Z. Biodegradable Soy Protein Isolate-Based Materials: A Review. Biomacromolecules 2011;12:3369–80.

[5] Fernández-Espada L, Bengoechea C, Cordobés F, Guerrero A. Thermomechanical properties and water uptake capacity of soy protein-based bioplastics processed by injection molding. J Appl Polym Sci 2016;133.

[6] Peng IC, Quass DW, Dayton WR, Allen CE. The physicochemical and functional-properties of soybean 11s globulin - a Review. Cereal Chem 1984;61:480–90.

[7] Lakemond CMM, de Jongh HHJ, Hessing M, Gruppen H, Voragen AGJ. Soy glycinin: Influence of pH and ionic strength on solubility and molecular structure at ambient temperatures. J Agric Food Chem 2000;48:1985–90.

[8] Kumar P, Sandeep KP, Alavi S, Truong VD, Gorga RE. Effect of Type and Content of Modified Montmorillonite on the Structure and Properties of Bio-Nanocomposite Films Based on Soy Protein Isolate and Montmorillonite. J Food Sci 2010;75:N46–56.

[9] Bagheri Marandi G, Mahdavinia GR, Ghafary S. Swelling behavior of novel protein-based superabsorbent nanocomposite. J Appl Polym Sci 2011;120:1170–9.

[10] Chivrac F, Pollett E, Schmutz M, Averous L. New approach to elaborate exfoliated starch-based nanobiocomposites. Biomacromolecules 2008;9:896–900.

[11] Dianez I, Martínez I, Partal P. Synergistic effect of combined nanoparticles to elaborate exfoliated egg-white protein-based nanobiocomposites. Compos Part B Eng 2016;88:36–43.

[12] Tee T-T, Sin LT, Gobinath R, Bee S-T, Hui D, Rahmat AR, et al. Investigation of nano-size montmorillonite on enhancing polyvinyl alcohol–starch blends prepared via solution cast approach. Compos Part B Eng 2013;47:238–47.

[13] Martino L, Guigo N, van Berkel JG, Sbirrazzuoli N. Influence of organically modified

montmorillonite and sepiolite clays on the physical properties of bio-based poly(ethylene 2,5-furandicarboxylate). Compos Part B Eng 2017;110:96–105. doi:https://doi.org/10.1016/j.compositesb.2016.11.008.

[14] Hernandez-Izquierdo VM, Krochta JM. Thermoplastic processing of proteins for film formation - A review. J Food Sci 2008;73:R30–9.

[15] Yang Y, Zhu ZK, Yin J, Wang XY, Qi ZE. Preparation and properties of hybrids of organo-soluble polyimide and montmorillonite with various chemical surface modification methods. Polymer (Guildf) 1999;40:4407–14.

[16] Hoyos CG, Vázquez A. Flexural properties loss of unidirectional epoxy/fique composites immersed in water and alkaline medium for construction application. Compos Part B Eng 2012;43:3120–30.

[17] A.O.A.C. Official Methods of Analysis. E.E.U.U.: Association of Official Analytical Chemist; 2000.

[18] Tummala P, Liu W, Drzal LT, Mohanty AK, Misra M. Influence of plasticizers on thermal and mechanical properties and morphology of soy-based bioplastics. Ind Eng Chem Res 2006;45:7491–6.

[19] Fang Y, Zhang B, Wei Y. Effects of the specific mechanical energy on the physicochemical properties of texturized soy protein during high-moisture extrusion cooking. J Food Eng 2014;121:32–8.

[20] Chen P, Zhang L. Interaction and Properties of Highly Exfoliated Soy Protein/Montmorillonite Nanocomposites. Biomacromolecules 2006;7:1700–6.

[21] ISO U-E. Plastics - Determination of tensile properties - Part 2: Test conditions for moulding and extrusion plastics 2012;527–2.

[22] Standard A. Standard Test Method for Tensile Properties of Plastics 2010;D638.

[23] ASTM. Standard test Method for Water Absorption of Plastics 2001;D570.

[24] De Rosa C, Auriemma F. Crystals and Crystallinity in Polymers: Diffraction Analysis of Ordered and Disordered Crystals. Wiley; 2013.

[25] Amr IT, Al-Amer A, P ST, Al-Harthi M, Girei SA, Sougrat R, et al. Effect of acid

treated carbon nanotubes on mechanical, rheological and thermal properties of polystyrene nanocomposites. Compos Part B Eng 2011;42:1554–61.

[26] Fernandez M, Landa M, Eugenia Munoz M, Santamaria A. Thermal and Viscoelastic Features of New Nanocomposites Based on a Hot-Melt Adhesive Polyurethane and Multi-Walled Carbon Nanotubes. Macromol Mater Eng 2010;295:1031–41.

[27] Landa M, Fernandez M, Munoz ME, Santamaria A. The Effect of Flow on the Physical Properties of Polyurethane/Carbon Nanotubes Nanocomposites: Repercussions on Their Use as Electrically Conductive Hot-Melt Adhesives. Polym Compos 2015;36:704–12.

[28] Feng JY, Chan CM, Li JX. A method to control the dispersion of carbon black in an immiscible polymer blend. Polym Eng Sci 2003;43:1058–63.

[29] Miriyala SM, Kim YS, Liu L, Grunlan JC. Segregated Networks of Carbon Black in Poly(vinyl acetate) Latex: Influence of Clay on the Electrical and Mechanical Behavior. Macromol Chem Phys 2008;209:2399–409.

[30] Wik VM, Aranguren MI, Mosiewicki MA. Castor Oil-based Polyurethanes Containing Cellulose Nanocrystals. Polym Eng Sci 2011;51:1389–96.

[31] Fernandez M, Landa M, Eugenia Munoz M, Santamaria A. Electrical conductivity of PUR/MWCNT nanocomposites in the molten state, during crystallization and in the solid state. Eur Polym J 2011;47:2078–86.

[32] Deutscher G, Kapitulnik A, Rappaport M. Percolation Structures and Processes. New York: Annals of the Israel Physical Society, American Institute of Physics; 1983.

[33] Ferry JD. Viscoelastic properties of polymers. Wiley; 1980.

[34] Guillard V, Chevillard A, Gastaldi E, Gontard N, Angellier-Coussy H. Water transport mechanisms in wheat gluten based (nano) composite materials. Eur Polym J 2013;49:1337–46.

[35] Angellier-Coussy H, Gastaldi E, Da Silva FC, Gontard N, Guillard V. Nanoparticle size and water diffusivity in nanocomposite agro-polymer based films. Eur Polym J 2013;49:299–306.

[36] Madyan OA, Fan M, Feo L, Hui D. Physical properties of clay aerogel composites: An

overview. Compos Part B Eng 2016;102:29–37.

[37] Stigter D, Dill KA. Charge effects on folded and unfolded proteins. Biochemistry 1990;29:1262–71.

[38] Prabakaran K, Mohanty S, Nayak SK. Solid state dye sensitized solar cells: Eosin-Y sensitized TiO2–ZnO/PEO–PVDF-HFP-MMT electrolytes/MWCNT–Nafion® counter electrode. Ceram Int 2015;41:11824–35.

[39] Balme S, Guegan R, Janot J-M, Jaber M, Lepoitevin M, Dejardin P, et al. Structure, orientation and stability of lysozyme confined in layered materials. Soft Matter 2013;9:3188–96.

[40] Chung Y-L, Ansari S, Estevez L, Hayrapetyan S, Giannelis EP, Lai H-M. Preparation and properties of biodegradable starch–clay nanocomposites. Carbohydr Polym 2010;79:391–6.

Figures

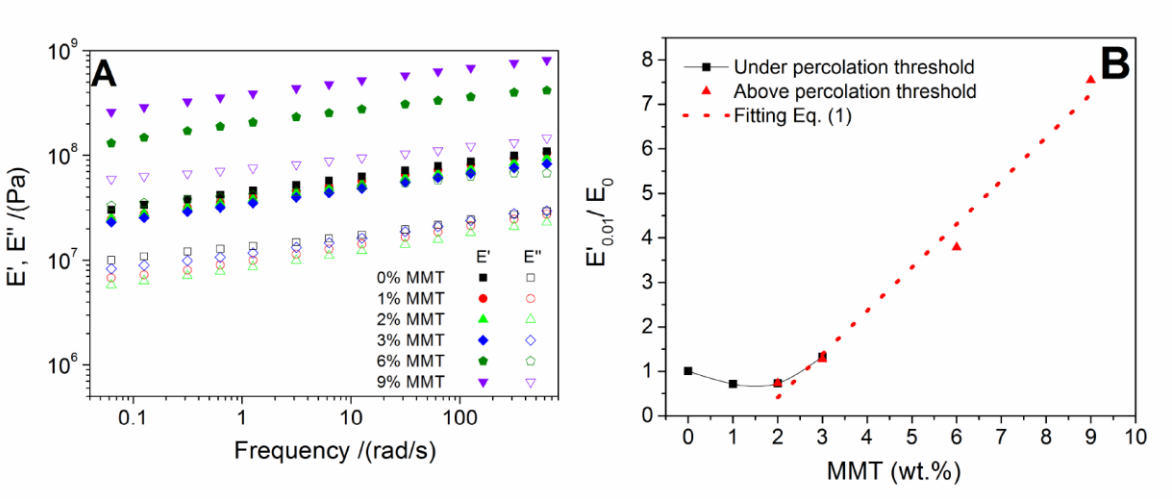

Figure 1. Mechanical spectra for the reference system: SPI-based bioplastic containing 0 % wt. MMT-Na^+ and containing different amounts of MMT-Na^+ (1, 2, 3, 6, 9 wt. %) (A) and the effect of MMT-Na^+ concentration on the elastic modulus, where E' is taken at the lowest values of the frequency (0.01Hz) divided by the lowest value of the elastic modulus for the reference system, E^0 ($E'_{0.01}/E^0$). This figure also shows the best fits of the data to Eq. (2) (B).

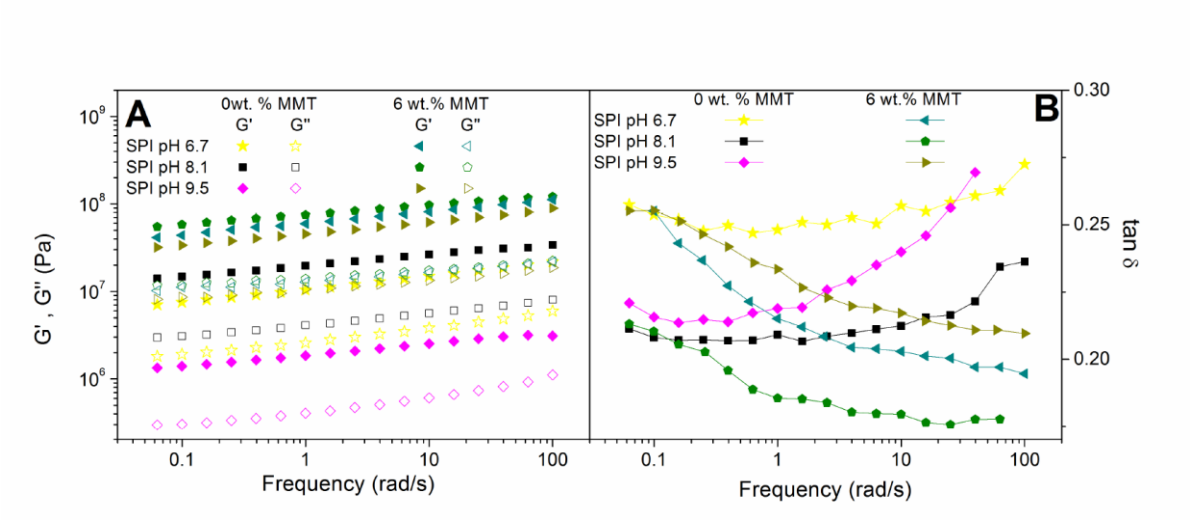

533

534 **Figure 2.** Mechanical spectra (A) and tan δ (B) for systems at different GL pH (acid,

535 native and basic) without MMT-Na^+ and containing 6 wt. % MMT-Na^+.

536

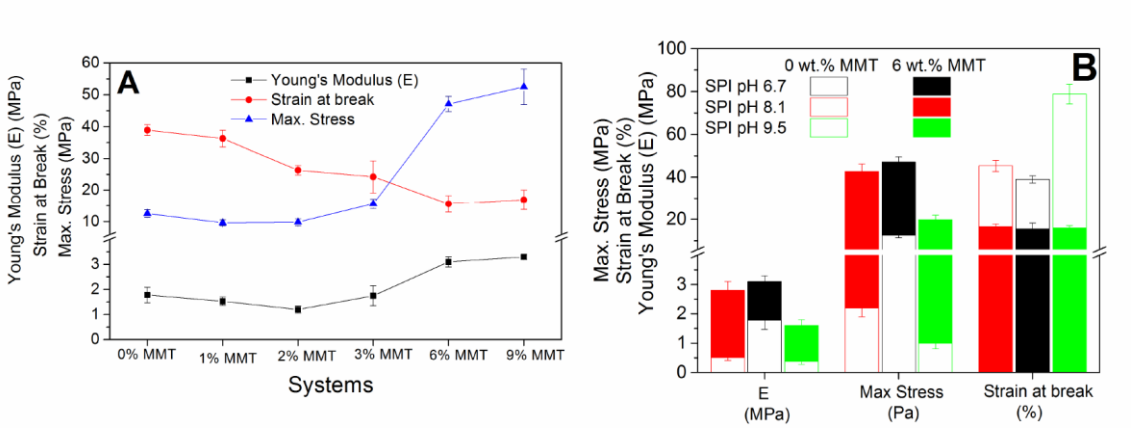

537

538 **Figure 3.** Parameters from tensile strength measurements: Max. stress, strain at break
539 and Youngs' Modulus (E) obtained from stress-strain curve for nanocomposites
540 containing different amounts of MMT-Na^+ (1, 2, 3, 6, 9 wt. %) (A), and for systems at
541 different GL pH (acid, native and basic) without MMT-Na^+ and containing 6 wt. % MMT-
542 Na^+ (B).

543

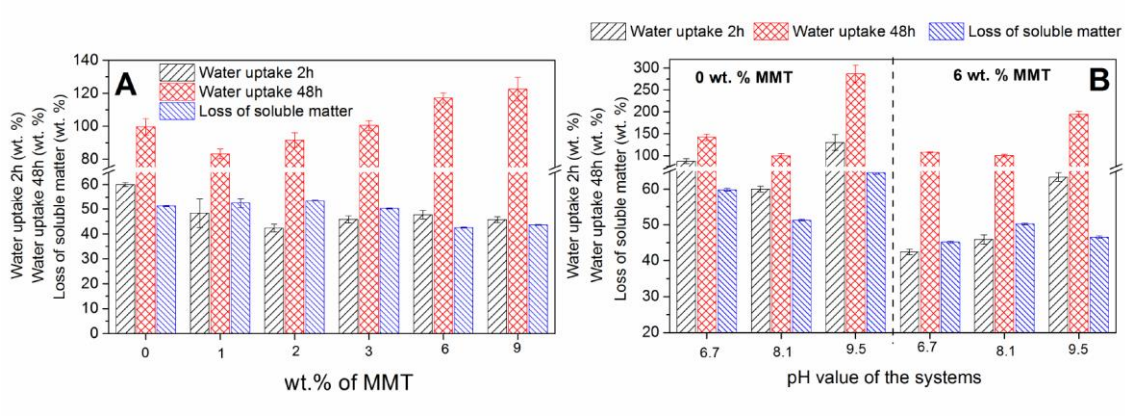

544

545 **Figure 4.** Evolution of water absorption capacity (%) after immersion for 2 h and 48 h,
546 as well as loss of soluble matter (%) for nanocomposites containing different amounts
547 of MMT-Na^+ (1, 2, 3, 6, 9 wt. %) (A), and for systems at different GL pH (acid, native
548 and basic) without MMT-Na^+ and containing 6 wt. % MMT-Na^+ (B).

549

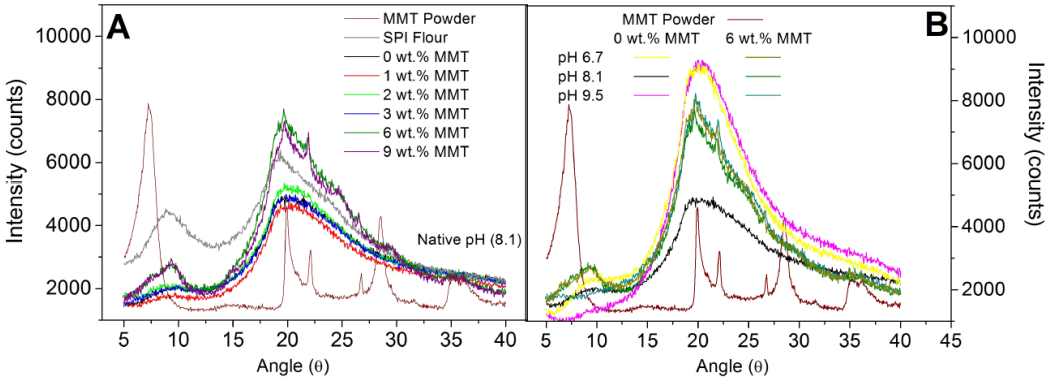

550

551 **Figure 5.** XRD for the protein powder, for the reference system: SPI-based bioplastic
552 containing 0 % wt. MMT-Na+ and for nanocomposites, containing different amounts of
553 MMT-Na+ (1, 2, 3, 6, 9 wt. %) (A), as well as for the native MMT-Na+ and for for
554 systems at different GL pH (acid, native and basic) without MMT-Na^+ and containing 6
555 wt. % MMT-Na^+ (B).

556

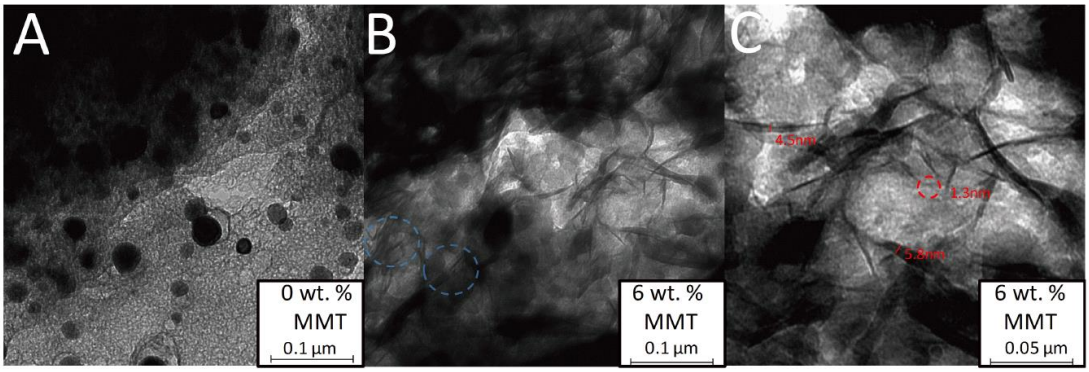

557

558 **Figure. 6** TEM images obtained from samples without MMT (A), as well as with MMT

559 (B and C).

560

Table

System	Extruder zone										
	1	2	3	4	5	6	7	8	9	10	Die
Temperature (^{0}C)	30	35	45	45	45	60	80	80	80	80	110

Table 1. Temperature profile for SPI-based extruded nanocomposites